Acta Neuropathol (2001) 101:555–564
DOI 10.1007/s004010000320

REGULAR PAPER

U. Rüb · K. Del Tredici · C. Schultz · D. R. Thal
E. Braak · H. Braak

The autonomic higher order processing nuclei of the lower brain stem are among the early targets of the Alzheimer's disease-related cytoskeletal pathology

Received: 30 June 2000 / Revised, accepted: 25 September 2000 / Published online: 21 June 2001

Abstract The nuclei of the pontine parabrachial region (medial parabrachial nucleus, MPB; lateral parabrachial nucleus, LPB; subpeduncular nucleus, SPP) together with the intermediate zone of the medullary reticular formation (IRZ) are pivotal relay stations within central autonomic regulatory feedback systems. This study was undertaken to investigate the evolution of the Alzheimer's disease-related cytoskeletal pathology in these four sites of the lower brain stem. We examined the MPB, LPB, SPP and IRZ in 27 autopsy cases and classified the cortical Alzheimer-related cytoskeletal anomalies according to an established staging system (neurofibrillary tangle/neuropil threads [NFT/NT] stages I–VI). The lesions were visualized either with the antibody AT8, which is immunospecific for the abnormally phosphorylated form of the cytoskeletal protein tau, or with a modified Gallyas silver iodide stain. The MPB, SPB, and IRZ display cytoskeletal pathology in stage I and the LPB in stage II, whereby bothstages correspond to the preclinical phase of Alzheimer's disease (AD). In stages III–IV (incipient AD), the MPB and SPP are severely affected. In all of the stage III–IV cases, the lesions in the LPB and IRZ are well developed. In stages V and VI (clinical phase of AD), the MPB and SPP are filled with the abnormal intraneuronal material. At stages V–VI, the LPB is moderately involved and the IRZ shows severe damage. The pathogenesis of the AD-related cytoskeletal lesions in the nuclei of the pontine parabrachial region and in the IRZ conforms with the cortical NFT/NT staging sequence I–VI. In the event that the cytoskeletal pathology observed in this study impairs the function of the nerve cells involved, it is conceivable that autonomic mechanisms progressively deteriorate with advancing cortical NFT/NT stages. This relationship remains to be established, but it could provide insights into the illusive correlation between the AD-related cytoskeletal pathology and the function of affected neurons.

Keywords Alzheimer's disease · Autonomic system · Cytoskeletal pathology · NFT/NT staging · Tau protein

Introduction

From a cytopathological standpoint, the "calling cards," so to speak,of Alzheimer's disease (AD) are the intraneuronal neurofibrillary tangles (NFTs) and neuropil threads (NTs). These solid bundles of non-soluble fibril networks have their pathogenesis in anomalies of the neuronal cytoskeleton caused by the abnormally phosphorylated form of the cytoskeletal protein tau [5, 18, 29, 43]. Accompanying abnormalities, i.e., the extracellular deposition of the protein β-amyloid, evolve independently [7, 9].

The abnormal tau protein appears in immunoreactions with the antibody AT8 at first as an evenly distributed non-argyrophilic material in the neuronal cell processes and somata of involved nerve cells [5, 18, 19, 30, 43]. Aggregation of this material presumably results in solid argyrophilic fiber bundles. The latter present in the somata as NFTs and in dendrites as NTs [8, 16, 18, 28, 43]. Cross-sectional studies reveal that AD-related cytoskeletal pathology within the cerebral cortex follows a specific pattern which displays only little inter-patient variation and passes through six NFT/NT stages [7, 9, 26].

At present, AD is a progressive degenerative disorder of the human brain capable of being diagnosed only when patients are in the final stages of the disease [42]. In spite of intense research efforts on multiple fronts, tangible progress towards development of effective early diagnostic and monitoring strategies for AD patients based on neuropsychological testing methods remains elusive [42, 50].

Although, in the search for such clinical parameters, it is legitimate to check the functional integrity of brain

Professor Eva Braak passed away on 25 August 2000.

U. Rüb (✉) · K. Del Tredici · C. Schultz · D.R. Thal · E. Braak
H. Braak
Department of Clinical Neuroanatomy,
Johann Wolfgang Goethe University
Theodor-Stern-Kai 7, 60590 Frankfurt/Main, Germany
e-mail: U.Rueb@em.uni-frankfurt.de,
Tel.: +49-69-63016916, Fax: +49-69-63016425

stem nuclei known to be involved in AD by administering clinical or neurophysiological tests [17, 25, 36, 39, 51], it remains to be determined neuropathologically whether the brain stem nuclei involved in specific autonomic CNS functions are among the early targets of the AD-related cytoskeletal pathology at all and, if so, whether the development of the interneuronal lesions in these nuclei correlates with the progression of the six cortical NFT/NT stages that reflect the clinical progression of the illness [2, 7, 9].

Neuropathologists have known since the late eighties that the nuclei of the pontine parabrachial region (medial parabrachial nucleus, MPB; lateral parabrachial nucleus, LPB; subpeduncular pigmented nucleus, SPP) are among the victims of the neurofibrillary tangle pathology [17, 36]. We know that all three of the aforementioned nuclei are vital relay stations within central autonomic neuronal circuits [3, 11, 20, 22, 36, 40]. Closely connected with the nuclei of the pontine parabrachial region is the intermediate zone of the medullary reticular formation (IRZ), the central autonomic region of the medulla oblongata [24, 33, 40]. Although AD-related NFTs/NTs have been documented in the medullary reticular formation previously [29, 54], it has not yet been shown whether the intermedi-

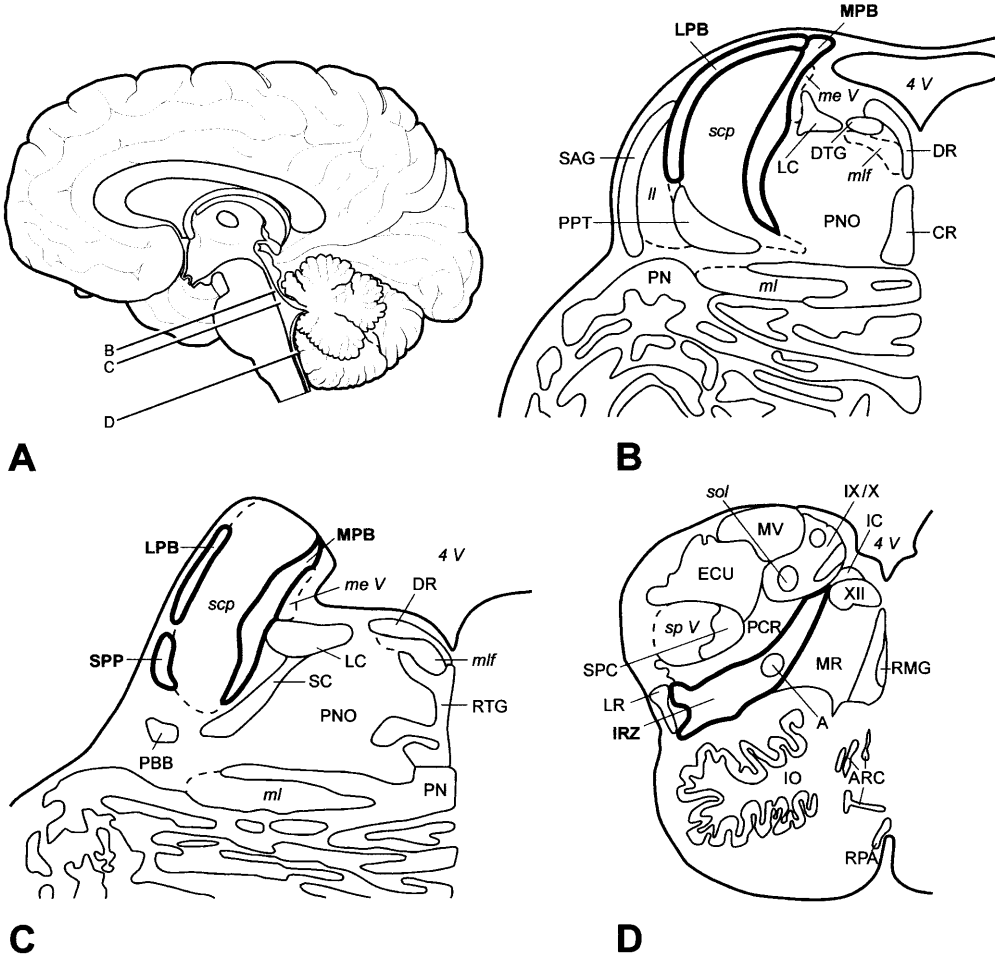

Fig. 1 **A** Median view of a mediosaggital section through the human brain. The *lines* drawn through the brain stem indicate the sectional plane of the frontal sections presented in **B**–**D** (*line B* sectional plane of the section in **B**, *line C* sectional plane of the section in **C**, *line D* sectional plane of the section in **D**). **B**–**D** Schematized frontal sections cut perpendicular to the brain stem axis of Meynert showing the nuclei of the pontine parabrachial region and the IRZ outlined by *bold lines* (for orientation, see **A**). **B** Rostral pons with the rostral portions of the LPB and the rostral portions of the MPB. **C** Rostral pons with the caudal portions of the LPB, the caudal portions of the MPB, and the SPP. **D** Medulla oblongata with the caudal portions of the IRZ (*A* ambiguus nucleus, *ARC* arcuate nucleus, *CR* central raphe nucleus, *DR* dorsal raphe nucleus, *DTG* dorsal tegmental nucleus [nucleus of Gudden], *ECU* external cuneate nucleus, *IC* intercalated nucleus of the medulla oblongata, *IO* inferior olive, *IRZ* intermediate zone of the medullary reticular formation, *LC* locus coeruleus, *ll* lateral lemniscus, *LPB* lateral parabrachial nucleus, *LR* lateral reticular nucleus, *me V* mesencephalic trigeminal tract, *ml* medial lemniscus, *mlf* medial longitudinal fascicle, *MPB* medial parabrachial nucleus, *MR* medial nucleus of the medullary reticular formation, *MV* medial vestibular nucleus, *PBB* pontobulbar body, *PCR* parvocellular reticular nucleus, *PN* pontine nuclei, *PNO* pontine reticular formation, oral nucleus, *PPT* pedunculopontine tegmental nucleus, *RMG* raphe magnus nucleus, *RPA* raphe pallidus nucleus, *RTG* reticulotegmental nucleus of the pons [nucleus of Bechterew], *SAG* sagulum, *SC* subcoeruleus nucleus, *scp* superior cerebellar peduncle, *sol* solitary tract, *SPC* spinal trigeminal nucleus, *sp V* spinal trigeminal tract, *SPP* subpeduncular pigmented nucleus, *4 V* fourth ventricle, *IX/X* dorsal glossopharyngeal and vagal area, *XII* hypoglossal nucleus)

ate zone is involved in the neurofibrillary cytoskeletal pathology.

As such, this study had two aims: First, to determine at what point in time the three nuclei of the pontine parabrachial region show the initial signs of AD-related cytoskeletal pathology and whether the latter conforms with the developmental stages of the lesions as they are known to us from the cerebral cortex. Second, we wanted to see whether and in which of the six cortical stages the IRZ becomes affected by the cytoskeletal lesions.

Anatomical remarks

The nuclei of the pontine parabrachial region include the MPB, LPB together with the SPP. All three are situated in the rostral portions of the pons and encircle the superior cerebellar peduncle (Fig. 1A–D) [11, 36, 38, 40]. Rostrally, the nuclei of the pontine parabrachial region are replaced by the pedunculopontine nucleus and the sagulum (Fig. 1B). The former terminate at the caudal end of the superior cerebellar peduncle. With their afferent and efferent fiber tracts, these pontine nuclei link up medullary autonomic centers (e.g., the intermediate reticular zone, the dorsal glossopharyngeal and vagal area) with telencephalic autonomic centers (e.g., amygdala, hypothalamus) [3, 11, 20, 22, 24, 33, 35, 40].

The demarcation lines of the IRZ were defined in 1986. In frontal sections through the lower brain stem, the IRZ appears as an oblique band of nerve cells which sweeps arch-like through the medulla oblongata (Fig. 1D). Dorsally, both the rostral and the caudal parts of the IRZ abut on the glossopharyngeal and vagal area, and in so doing harbor the ambiguus nucleus (Fig. 1D). The rostral portions of the IRZ are situated laterally from the gigantocellular reticular nucleus, medially from the parvocellular reticular nucleus, and extend nearly to the surface of the medulla oblongata. The caudal portions separate the medial reticular nucleus from the laterally situated dorsal reticular nucleus and extend to the lateral reticular nucleus (Fig. 1D). The medium-sized fusiform nerve cells and triangular neuronsof the IRZ are oriented with their longitudinal axes parallel to the arch-like course of the IRZ [24, 33, 40]. The IRZ is a major link between the dorsal glossopharyngeal and vagal area and the nuclei of the parabrachial region. It is known as an important center of respiratory and cardiovascular autonomic activities [24, 33, 40].

Material and methods

We investigated 27 cases at autopsy (16 females, mean age 80.1± 6.8 years; 11 males, mean age 78.7±8.7 years). Following fixation in a 4% aqueous formaldehyde solution, the brain stems of all 27 cases were severed perpendicular to the brain stem axis of Meynert at the level of the inferior colliculus. Blocks of tissue excised from the hemispheres were embedded in polyethylene glycol (PEG 1000, Merck) and cut perpendicular to the intercommissural axis into uninterrupted series of 100 µm sections. The brain stems were not dissected further, but rather dehydrated *in toto*, embedded in PEG, and microtomed into unbroken series of 100 µm frontal sections [7, 52].

On the 1st, 11th, 21st, etc. of these serial sections, which were stained with aldehyde-fuchsin Darrow red [7], we defined the borders of the LPB, the MPB, the SPP and the IRZ [24, 33, 36, 38, 40]. We stained the 2nd,12th, 22nd, etc. sections of these series with the modified Gallyas silver iodide technique to ascertain the presence of AD-related neurofibrillary pathology [8, 16, 28]. The 3rd, 13th, 23rd, etc. sections of all series were stained with the Campbell-Switzer silver-pyridine technique for identifying deposits of the protein β-amyloid. Finally, we treated the 4th, 14th, 24th, etc. of the serial sections from 24 selected cases with the monoclonal antibody AT8 to visualize existing abnormal cytoskeletal tau protein (Innogenetics, Ghent, Belgium; dilution 1: 2000) [5, 19, 34]. The free-floating brain stem sections were incubated for about 40 h at 4°C after application of the antibody AT8. Following processing with the second biotinylated antibody (anti-mouse IgG, 2 h) immunoreactions were visualized with the ABC complex (Vectastain) and 3,3'-diaminobenzidine-tetrahydrochloride/H_2O_2 (DAB, D5637 Sigma). This set of sections from 7 cases was counterstained with aldehyde-fuchsin Darrow red.

All of the cases were classified using parameters of the AD staging procedure, which differentiates six stages (I–VI) of increasingly severe cortical neurofibrillary pathology and three stages (A–C) in the evolution of intracerebral β-amyloid deposits [7, 9] (Table 1). In each instance, an average of six Gallyas-stained, six Campbell-Switzer-stained, and immunohistochemically treated frontal sections from the pontine parabrachial region and IRZ were evaluated semiquantitativelyto determine the severity of the AD-related neurofibrillary pathology and that of the AT8-immunoreactive cytoskeletal pathology. All tissue sections assessed were done so blinded to the above-mentioned AD staging results.

With the help of the one-way analysis of variance according to Kruskal and Wallis (H-test), we looked to see if the severity of the AT8-immunoreactive material as well as that of the AD-related neurofibrillary lesions in the four sites under discussion were dependent upon the stages I–VI. We tested our *a priori* working hypothesis to the effect that the severity of the AT8-immunopositive alterations and that of the AD-related neurofibrillary pathology in the four brain stem structures selected for this study increase stage for stage with the severity of cortical neurofibrillary pathology by means of a nonparametric trend analysis. With the help of Kendall's rank correlation coefficient tau (τ), we described the relationship between the severity of the immunopositive cytoskeletal lesions and that of the neurofibrillary pathology [4].

Results

AT8-immunoreactive cytoskeletal alterations in the nuclei of the parabrachial pontine region

In all of the cortical NFT/NT stage I cases (i.e., the preclinical phase of AD) investigated in this study, the MPB and SPP display some AT8-immunopositive cellular processes and somata (Table 1, Fig. 2A). The LPB likewise exhibits AT8-immunopositive somata and cellular processes in cases with preclinical stages. In this nuclear gray, the immunopositive material appears consistently in cases at cortical stage II (Table 1). In all three nuclei, the severity of the AT8-immunoreactive cytoskeletal alterations increases in cortical stages III–IV (Table 1, Fig. 2B). In these stages, the severity of the immunopositive cytoskeletal lesions is clearly higher in the MPB and SPP than in the LPB (Table 1). In all cortical stage V and VI cases studied, the MPB and SPP display an abundance of AT8-immunopositive somata located within a dense weave of

Table 1 Summary of AD-related cytoskeletal alterations in the nuclei of the pontine parabrachial region and in the IRZ at cortical NFT/NT stages I–VI together with β-amyloid stages (0–C). For each nucleus (MPB, LPB, SPP, IRZ), the semiquantitatively determined severity of the neurofibrillary pathology (NFTs/NTs), severity of AT8-immunopositive cytoskeletal alterations (*0* none, *1* sparse, *2* moderate, *3* marked, *4* severe, – not determined), and the median and range of the severity of neurofibrillary and AT8-immunopositive lesions for each stage are given (*AD* Alzheimer's disease, *MPB* medial parabrachial nucleus, *LPB* lateral parabrachial nucleus, SPP subpeduncular pigmented nucleus, *IRZ* intermediate zone of the medullary reticular formation, *NFT* neurofibrillary tangle, *NT* neuropil thread)

Case	Age	Sex	β-Amyloid	MPB		LPB		SPP		IRZ	
				NFTs/NTs	AT8	NFTs/NTs	AT8	NFTs/NTs	AT8	NFTs/NTs	AT8
Stage I											
1	57	M	0	0	1	0	0	0	1	0	1
2	73	F	0	0	1	0	1	0	1	0	1
3	77	M	0	1	2	0	0	0	1	0	1
4	79	M	0	1	1	0	0	0	1	0	1
5	80	F	0	1	1	0	1	0	1	0	1
Median				1	1	0	0	0	1	0	1
Range				1	1	0	1	0	0	0	0
Stage II											
6	73	M	0	1	2	1	1	0	1	1	1
7	75	F	0	0	1	0	1	0	2	1	2
8	77	M	0	0	2	0	1	0	2	1	1
9	80	M	0	1	2	0	1	0	1	1	1
10	88	M	0	1	2	0	1	1	2	1	2
Median				1	2	0	1	0	2	1	1
Range				1	1	1	0	1	1	0	1
Stage III											
11	76	F	B	2	2	1	1	1	2	1	2
12	79	F	B	1	–	1	–	1	–	1	–
13	79	M	B	1	–	1	–	2	–	2	–
14	83	M	0	2	3	1	1	1	3	1	2
15	84	M	B	2	3	1	1	2	3	2	2
Median				2	3	1	1	1	3	1	2
Range				1	1	0	0	1	1	1	0
Stage IV											
16	78	F	C	3	3	1	2	3	3	1	2
17	78	F	C	4	4	1	2	3	4	2	3
18	88	F	B	3	3	1	2	3	3	2	2
19	90	F	0	3	3	1	2	2	3	2	2
Median				3	3	1	2	3	3	2	2
Range				1	1	0	0	1	1	1	1
Stage V											
20	69	F	C	4	4	2	2	4	4	3	3
21	80	F	C	3	4	2	2	3	3	2	3
22	85	F	C	3	4	2	2	3	4	3	3
23	85	F	C	3	3	2	2	3	3	2	3
24	86	F	C	4	4	2	2	4	4	3	3
25	89	M	C	3	4	2	2	3	4	3	3
Median				3	4	2	2	3	4	3	3
Range				1	1	0	0	1	1	1	0
Stage VI											
26	69	F	C	3	4	2	2	3	4	3	3
27	91	F	C	3	–	2	–	3	–	3	–
Median				3	4	2	2	3	4	3	3
Range				0	0	0	0	0	0	0	0

immunoreactive cellular processes (Table 1, Fig. 2C). In cortical stages V-VI, the LPB is moderately involved (Table 1, Fig. 2C). At all three sites, the severity of the immunoreactive alterations conforms with the progression of the cortical stages I to VI, a correlation characterized by a linear trend (Table 2).

AD-related neurofibrillary pathology in the nuclei of the parabrachial pontine region

In cortical stages I and II, only some cases display AD-related NFTs/NTs in the pontine parabrachial nuclei, whereas in cortical stage III, the MPB, LPB, and SPP routinely are affected by NFTs/NTs (Table 1). The severity of the

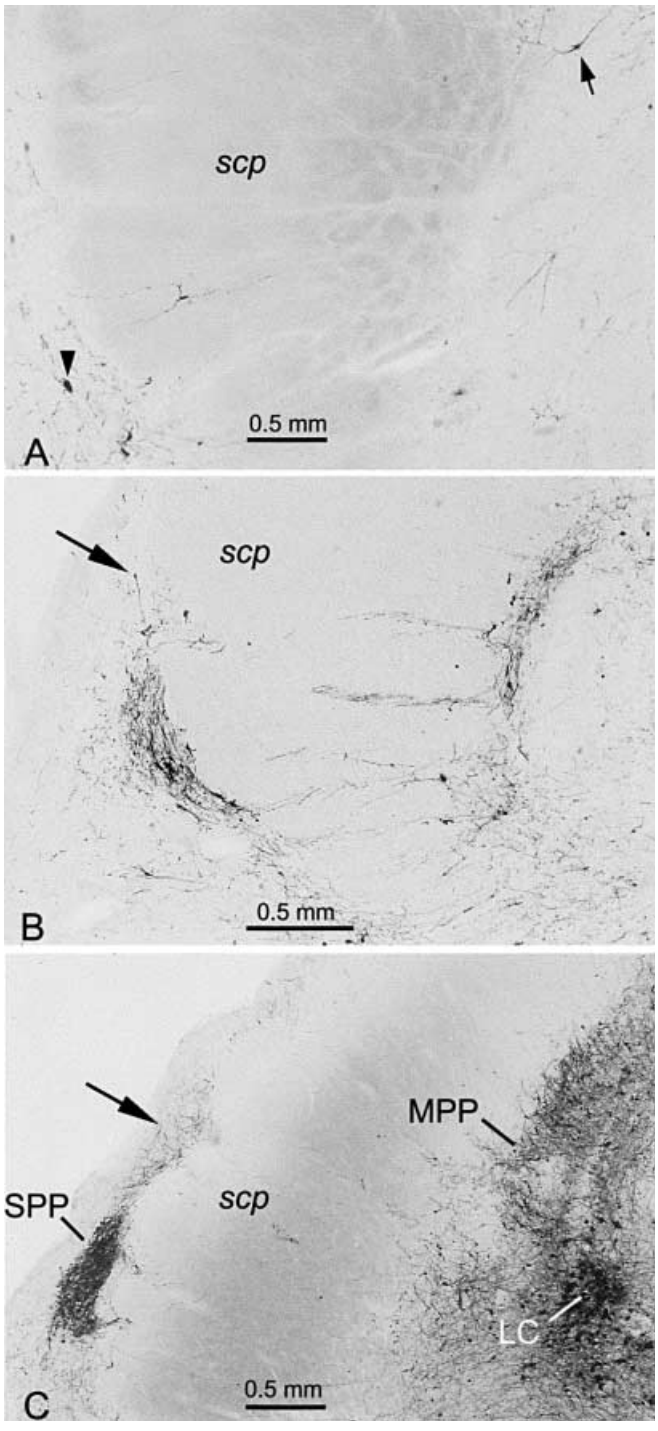

Fig. 2A–C AD-related immunopositive cytoskeletal alterations in the lower portions of MPB and LPB as well as in the SPP. *Elongated arrows* point to the cytoskeletal alterations in the LPB. *Arrow* indicates the cytoskeletal changes in the MPB. *Arrowhead* marks the lesions in the SPP. For topographical orientation, see Fig. 1C. **A** Initial degree of AT8-immunoreactive cytoskeletal pathology in the MPB and SPP in cortical NFT/NT stage I (case 5, Table 1). **B** Pronounced AT8-immunoreactive cytoskeletal anomalies in the MPB and SPP and slight alterations in the LBP of a representative case at cortical NFT/NT stage III (case 15, Table 1). **C** Severe AT8-immunoreactive cytoskeletal alterations are seen in the MPB and SPP, and moderate lesions are found in the LPB in cases at the cortical NFT/NT stage V (case 22, Table 1). (See also legend to Fig. 1). **A**–**C** PEG sections, AT8 immunostaining, 100 μm

Table 2 Results of the statistical analyses

	MPB	LPB	SPP	IRZ
AT8: H corr[a]	20.03	21.78	19.90	20.20
P	<0.005	<0.001	<0.005	<0.005
AT8: H lin[b]	9.32	7.67	9.53	8.56
P	<0.005	<0.01	<0.005	<0.005
NFTs/NTs: H corr[c]	22.63	25.17	24.00	22.91
P	<0.0005	<0.0005	<0.0005	<0.0005
NFTs/NTs: H lin[d]	12.03	13.92	13.86	16.21
P	<0.001	<0.0005	<0.0005	<0.0005
AT8–NFTs/NTs: τ[e]	0.83	0.76	0.86	0.83
P	<0.005	<0.005	<0.005	<0.005

[a]One-way analysis of variance for the AT8-immunopositive nerve cell somata and cellular processes
[b]Trend analyses for the AT8-immunopositive nerve cell somata and cellular processes
[c]One-way analysis of variance for the NFTs/NTs
[d]Trend analyses for the NFTs/NTs
[e]Kendall's rank correlation tau between the severity of AT8-immunopositive lesions and the severity of the neurofibrillary pathology

neurofibrillary pathology in all three nuclei still is mild in cortical stage III. As is the case with AT8-immunoreactive material, the severity of the neurofibrillary lesions at all three sites increases in cortical stages VI–VI and definitely is more pronounced in the MPB and SPP than in the LPB (Table 1). In cortical stages V and VI, the MPB and SPP are infested with NFTs/NTs, and the LPB exhibits moderate damage (Table 1; Fig. 3A, B). The severity of the neurofibrillary pathology in the three nuclei increases gradually with the growing severity of the AT8-immunopositive lesions (Table 2) and correlates significantly with the cortical stages I–VI. This correlation is characterized by a linear trend (Table 2).

AD-related β-amyloid deposits in the nuclei of the parabrachial pontine region

Deposition of the protein β-amyloid is seen only in 2 of 27 cases. These 2 cases are at stage C in the evolution of intracerebral β-amyloid deposits (cases 22 and 24, Table 1), which appear only in the medial parabrachial and subpeduncular nuclei in small numbers and contain no neuritic components.

AT8-immunoreactive cytoskeletal alterations in the IRZ

All cortical NFT/NT stages I–II cases investigated already display isolated AT8-immunopositive nerve cell somata and nerve cell processes (Table 1, Fig. 4A). In cases at cortical stages III–IV, the immunoreactive cytoskeletal pathology in the IRZ is more pronounced than in stages I–II (Table 1, Fig. 4B). At cortical stages V-VI, the IRZ typically shows marked immunoreactive cytoskeletal le-

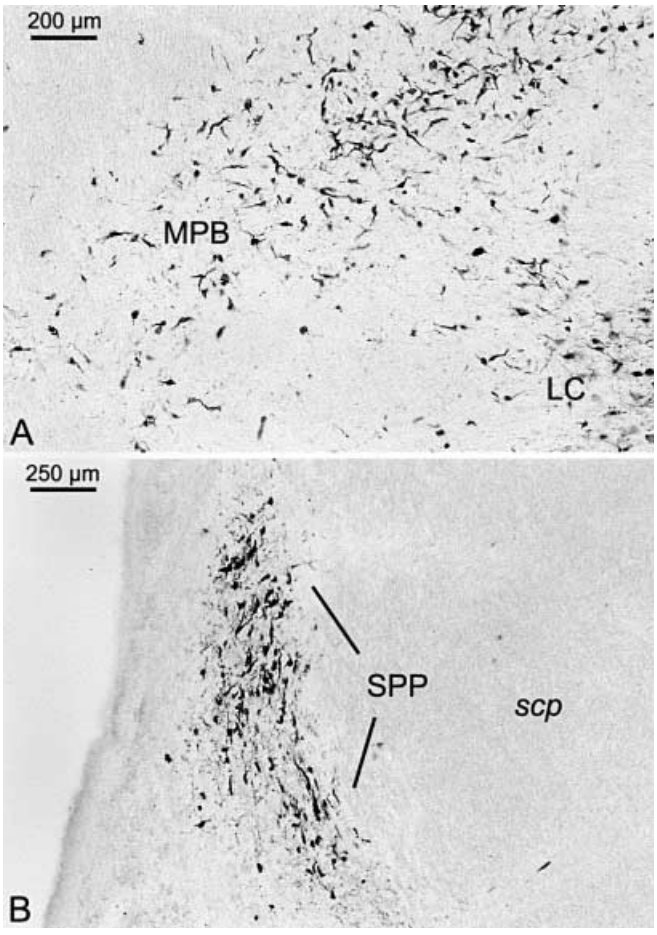

Fig. 3A, B AD-related NFTs/NTs in the nuclei of the pontine parabrachial region in cortical NFT/NT stage V. For topographical orientation, see Fig. 1C. Severe Gallyas-positive cytoskeletal pathology in the MPB (**A**) and in the SPP (**B**) in a typical case at cortical NFT/NT stage V (case 20, Table 1). **A**, **B** PEG sections, Gallyas silver iodide staining, 100 µm

sions (Table 1, Figs. 4C, 5). In these stages, large amounts of immunopositive neuronal somata and cellular processes cut an arch-shaped swath reaching from the dorsal glossopharyngeal-vagal area to the surface of the medulla oblongata rostrally and the lateral reticular nucleus caudally (Fig. 5). The severity of the immunoreactive lesions in the IRZ correlates with the progression of the cortical stages I–VI, and this correlation, like the immediately preceding one, is expressed by a linear trend (Table 2).

AD-related neurofibrillary pathology in the IRZ

The IRZ is consistently involved in the AD-related neurofibrillary pathology beginning in stage II (Table 1). At this stage, only isolated neurons in the IRZ display NFTs/NTs (Table 1). In stages III–IV, NFTs/NTs in the IRZ appear with ever greater prevalence (Table 1). In cortical stages V-VI, increasing numbers of nerve cells in the IRZ exhibit NFTs/NTs (Table 1). As such, it can be said that the severity of the neurofibrillary pathology in the IRZ increases linearly with that of the AT8-immunoreactive lesions present there – and this in correlation with the cortical stages I–VI (Table 2).

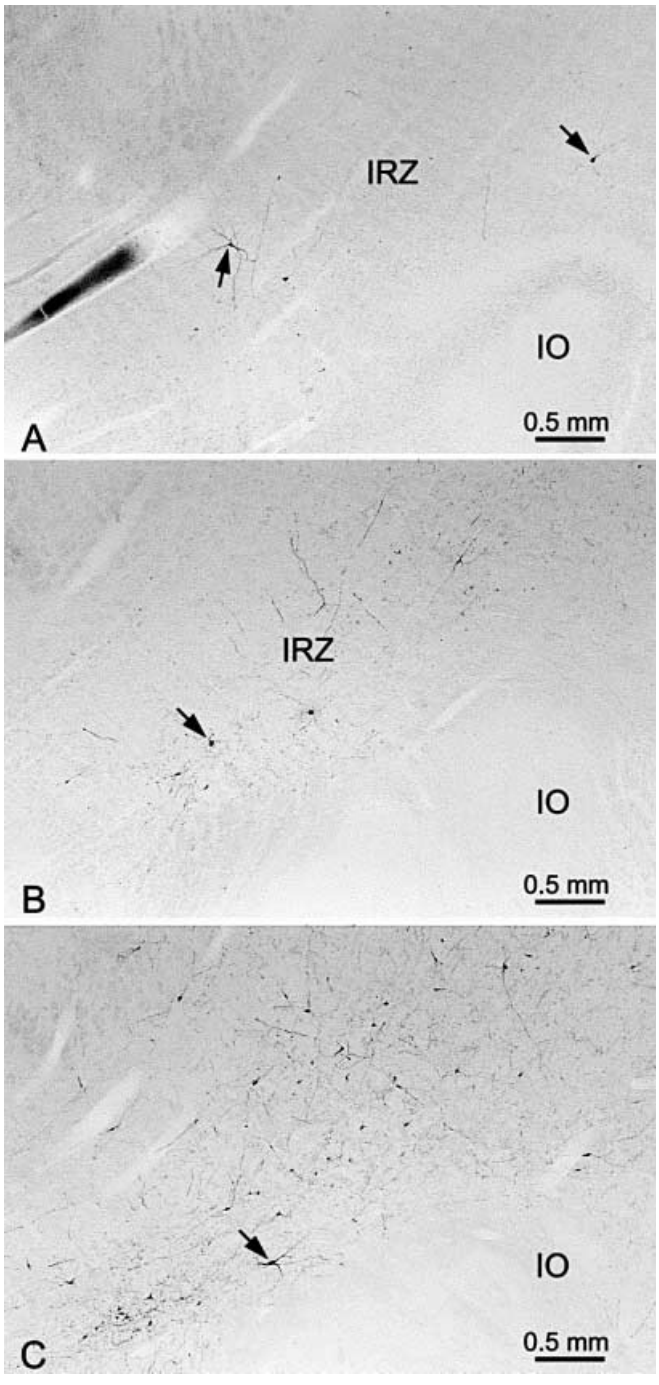

Fig. 4 AD-related immunopositive cytoskeletal alterations in the IRZ. *Arrows* indicate AD-related lesions in the IRZ. For topographical orientation, see Fig. 1D. **A** Slight AT8-immunoreactive cytoskeletal pathology in the IRZ in a typical cortical NFT/NT stage I case (case 2, Table 1). **B** Moderate AT8-immunoreactive cytoskeletal alterations of a case at cortical NFT/NT stage III (case 15, Table 1). **C** Marked AT8-immunoreactive changes occur in the IRZ in cases at cortical NFT/NT stage V (case 20, Table 1). **A**–**C** PEG sections, AT8 immunostaining, 100 µm

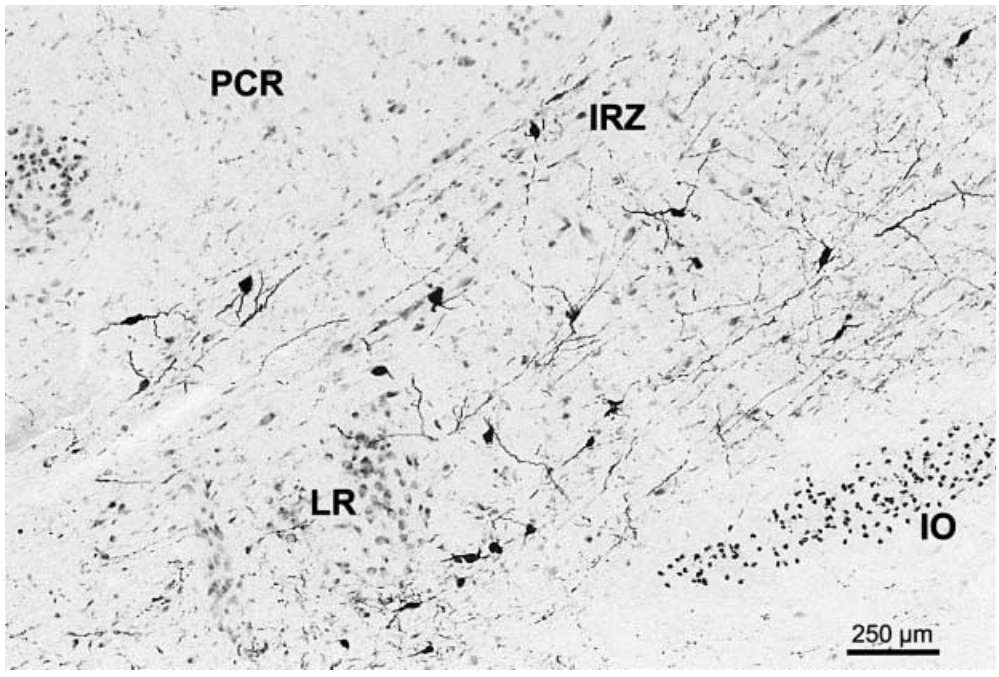

Fig. 5 Pronounced AD-related cytoskeletal pathology in the IRZ in cortical NFT/NT stage V (case 21, Table 1). For topographical orientation, see Fig. 1D, for abbreviations see legend to Fig. 1. PEG section, AT8 immunostaining and counterstaining with aldehyde-fuchsin Darrow red, 100 µm

AD-related β-amyloid deposits in the IRZ

The IRZ is completely devoid of β-amyloid deposits.

Discussion

Cytoskeletal anomalies emerge early in the nuclei of the pontine parabrachial region and IRZ. The development of the neurofibrillary pathology in the MPB, SPB, and IRZ commences already in cortical stage I and in the LPB in cortical stage II. At all four sites, the progression of the lesions correlates linearly with the NFT/NT cortical staging sequence I–VI (Fig. 6). This finding indicates, alongside of results from other studies in which subcortical nuclear grays have been analyzed for the presence of AD-related cytoskeletal lesions, that the NFT/NT stages I–VI most probably reflect not only the progress of the AD-related

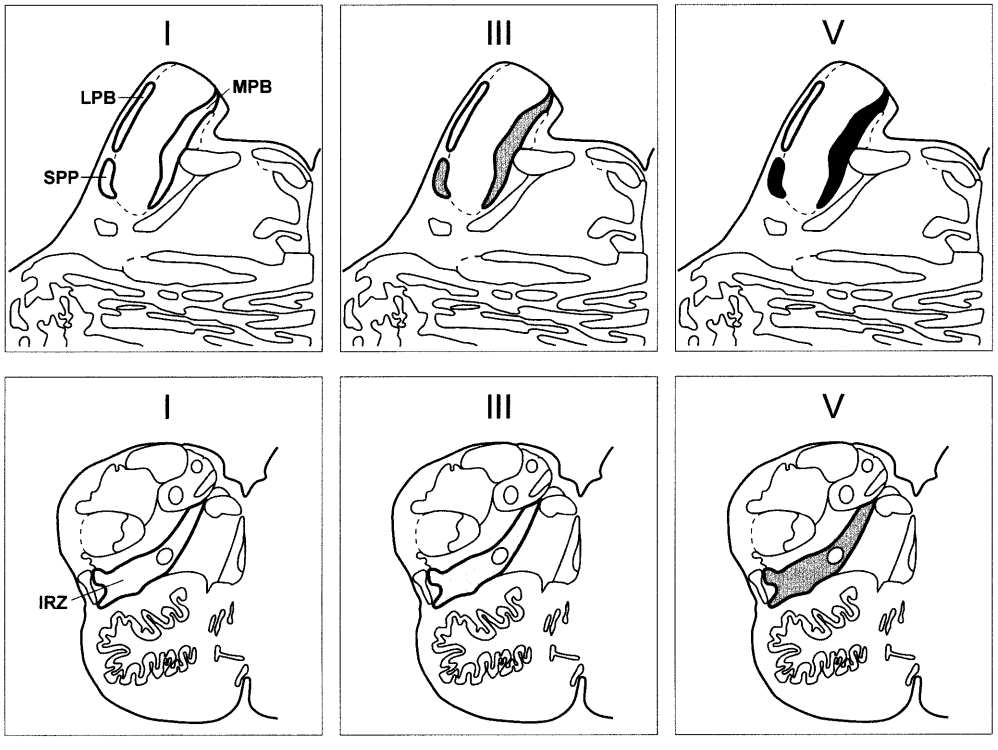

Fig. 6 Simplified diagrams summarizing the progression of the AD-related cytoskeletal pathology through cortical NFT/NT stages I, III, and V in the lower portions of the pontine parabrachial region and IRZ. The growing severity of the cytoskeletal pathology is indicated by increased densities of shading. *Upper row* Progression of the cytoskeletal alterations in the MPB, LPB, and SPP. *Lower row* Progression of the AD-related cytoskeletal pathology in the IRZ

cytoskeletal pathology in cortical areas but also its evolution in specific subcortical sites [7, 45, 49].

Our data show that the severity of the AT8-immunoreactive cytoskeletal alterations in the four lower brain stem sites selected for study correlates positively with the severity of the neurofibrillary pathology encountered there, whereby the antibody AT8 is capable of detecting the cytoskeletal alterations at earlier stages than the modified Gallyas silver iodide stain. Second, our findings reinforce the theory that the immunopositive intraneuronal material made visible with the antibody AT8 may serve as the basis for the formation of the argyrophilic intraneuronal fiber bundles underlying the AD-related neurofibrillary lesions [5, 18, 43].

β-amyloid deposits (for the first time in stage C) develop only in the MPB and SPP. Furthermore, they appear at both of these sites late and inconsistently. This would seem to indicate that the amyloid cascade hypothesis [21], which postulates that deposition of β-amyloid is required for the formation of the cytoskeletal pathology, is not universally applicable.

In our introduction, we already made reference to existing studies devoted to the pontine parabrachial region and its involvement in the AD cytoskeletal pathology [17, 36]. Parvizi et al. [39] subsequently called attention to the existence of greater numbers of AD-related cytoskeletal anomalies in the MPB and SPP than in the LPB, and our results substantiate the accuracy of their observations. The degree, however, of nerve cell density in the various regions of the LPB normally is considerably lower than that in the MPB or SPP, and there are no studies to date in which the density ratio of the affected neurons in the LPB has been determined.

Pending the results of such studies, therefore, it would be untenable to extrapolate from the mere observation that the LPB displays fewer AD-related cytoskeletal lesions to the conclusion that the LPB is less prone than the other two nuclei to develop the intraneuronal pathology. In fact, the onset of the cytoskeletal alterations in the LPB lags one stage behind that in the MPB and SPP. Accordingly, inasmuch as the duration of a single cortical NFT/NT stage is approximately 7–10 years [37], this lag time on the part of the LPB is presumably not inconsequential and constitutes a more plausible criterion than numerical prevalence for positing the greater resistance of LPB in the face of the AD-related neurofibrillary changes.

The distribution pattern of the intracerebral AD-related neurofibrillary lesions is typified by only minimal interindividual variations [7, 9]. In view of this fact, it is hardly conceivable that such a lesional distribution pattern is the product of pure coincidence. Scientists have always been fascinated by this problematic and have felt compelled to explain it [10, 13, 17, 41, 44, 48]. These authors [10, 13, 17, 41, 44, 48] view the anatomical connectivities of a given structure within the CNS as well as the degree to which the axons establishing these connectivities are myelinated as two important criteria for determining whether and when certain neuronal subtypes become targets of the cytoskeletal pathology. Although on ethical and methodological grounds it is impossible to demonstrate the validity of their criteria, their position can at least be backed up by empirical observation.

The entorhinal area and basal nucleus of Meynert, both of which display the AD-related cytoskeletal anomalies in cortical stages I–II very clearly and sustain heavy damage in stages III–VI [7, 9, 49], are among the destinationsof weakly myelinated efferent projections emerging from the pontine parabrachial nuclei [27, 46]. More importantly, the nuclei of the pontine parabrachial region and IRZ are reciprocally connected via axons equipped with, at best, thin myelin sheathes [35]. Together with the results of other studies [6, 17, 36, 39, 45, 49] our observationthat the nuclei of the pontine parabrachial region and the IRZ are among the early targets of the AD-related cytoskeletal pathology is in favor of the above-mentioned two-pronged hypothesis.

Various clinical studies have reported a noticeably higher incidence of cardiovascular and respiratory dysfunctions on the part of AD patients in comparison with others in their age groups [1, 15, 23, 32, 53]. The MPB, LPB, SPP, and IRZ are crucial relay stations within central autonomic feedback systems and vital participants in the regulation of cardiovascular and respiratory functions. Autonomic regulative deficits in AD may be linked to neuronal dysfunctions which originally were triggered by cytoskeletal alterations not only in autonomic centers of the forebrain [12, 14, 31, 47] but also in the MPB, LPB, SPP, and IRZ.

The development of the AD-related cytoskeletal pathology in the MPB, LPB, SPP, and IRZ fulfills all of the necessary criteria which legitimate further study of the possible functional consequences of these lesions. Together with the IRZ, which represents the predominant autonomic center of the human reticular formation, the nuclei of the pontine parabrachial nuclei are among the brain stem structures that become early targets of the AD-related cytoskeletal pathology. The severity of the pathology seen in the three nuclei ofthe pontine parabrachial region, like that seen in the IRZ, increases linearly with the staging sequence I–VI, which reflects the clinical course of the disorder [2, 7, 9].

In conclusion, it is conceivable that a progressive deterioration of cardiovascular and respiratory functions occurs with advancing cortical NFT/NT stages. This relationship remains to be established by large-scale and carefully monitored clinicopathological studies dealing with the following questions: (1) Do cardiovascular and respiratory dysfunctions occur already during the preclincial and clinically incipient phase of the AD? (2) If so, do they manifest themselves in all or in a majority of individuals in this phase of AD?(3) Finally, provided the first two questions can be answered affirmatively, should cardiovascular and respiratory system deficits be included in standardized clinical protocols of AD early symptoms with a view toward improved early diagnosis, and might not these same deficits serve as parameters for monitoring the clinical progression of the disease?

Acknowledgements. This work was supported by a research grant from the Deutsche Forschungsgemeinschaft. The skillful assistance of Ms. I. Szasz (graphics) is gratefully acknowledged. The authors thank J. Bohl and H. H. Goebel (Institute for Neuropathology, Mainz) for providing autopsy material.

References

1. Aharon-Peretz J, Harel T, Revach M, Ben-Haim SA (1992) Increased sympathetic and decreased parasympathetic cardiac innervation in patients with Alzheimer's disease. Arch Neurol 49:919–921
2. Bancher C, Braak H, Fischer P, Jellinger KA (1993) Neuropathological staging of Alzheimer lesions and intellectual status in Alzheimer's and Parkinson's patients. Neurosci Lett 162:179–182
3. Bernard JF, Bester H, Besson JM (1996) Involvement of the spino-parabrachio-amygdaloid and -hypothalamic pathways in the autonomic and affective emotional aspects of pain. Prog Brain Res 107:243–255
4. Bortz J, Lienert GA, Boehnke K (1990) Verteilungsfreie Methoden in der Biostatistik. Springer, Berlin Heidelberg New York
5. Braak E, Braak H, Mandelkow EM (1994) A sequence of cytoskeleton changes related to the formation of neurofibrillary tangles and neuropil threads. Acta Neuropathol 87:554–567
6. Braak H, Braak E (1991) Alzheimer's disease affects limbic nuclei of the thalamus. Acta Neuropathol 81:261–268
7. Braak H, Braak E (1991) Neuropathological stageing of Alzheimer-related changes. Acta Neuropathol 82:239–259
8. Braak H, Braak E (1991) Demonstration of amyloid deposits and neurofibrillary changes in whole brain sections. Brain Pathol 1:213–216
9. Braak H, Braak E (1995) Staging of Alzheimer's disease-related neurofibrillary changes. Neurobiol Aging 16:271–284
10. Braak H, Braak E (1996) Development of Alzheimer-related neurofibrillary changes in the neocortex inversely recapitulates cortical myelogenesis. Acta Neuropathol 92:197–201
11. Burstein R (1996) Somatosensory and visceral input to the hypothalamus and limbic system. Prog Brain Res 107:257–267
12. Chu CC, Tranel D, Damasio AR, Van Hoesen GW (1997) The autonomic-related cortex: pathology in Alzheimer's disease. Cereb Cortex 7:86–95
13. De Lacoste MC, White CL (1993) The role of cortical connectivity in Alzheimer's disease pathogenesis: a review and a model system. Neurobiol Aging 14:1–16
14. Esiri MM, Pearson RCA, Steele JE, Bowen DM, Powell TPS (1990) A quantitative study of the neurofibrillary tangles and the choline acetyltransferase activity in the cerebral cortex and the amygdala in Alzheimer's disease. J Neurol Neurosurg Psychiatry 53:161–165
15. Franceschi M, Ferini-Strambi L, Minicucci F, Sferazza-Papa A, Smirne S (1986) Signs of cardiac autonomic dysfunction during sleep in patients with Alzheimer's disease. Gerontology 32:327–334
16. Gallyas F (1971) Silver staining of Alzheimer's neurofibrillary changes by means of physical development. Acta Morphol Acad Sci Hung 19:1–8
17. German DC, White CL, Sparkman DR (1987) Alzheimer's disease: neurofibrillary tangles in nuclei that project to the cerebral cortex. Neuroscience 21:305–312
18. Goedert M (1993) Tau protein and the neurofibrillary pathology of Alzheimer's disease. Trends Neurosci 16:460–465
19. Goedert M, Jakes R, Vanmechelen E (1995) Monoclonal antibody AT8 recognises tau protein phosphorylated at both serine 202 and threonine 205. Neurosci Lett 189:167–170
20. Guyenet PG, Koshiya N, Huangfu D, Baraban SC, Stornetta RL, Li YW (1996) Role of medulla oblongata in generation of sympathetic and vagal outflows. Prog Brain Res 107:127–144
21. Hardy JA, Higgins GA (1992) Alzheimer's disease: the amyloid cascade hypothesis. Science 256:184–185
22. Harper RM, Rector D, Poe G, Frysinger RC, Kristensen M, Gozal D (1996) Rostral brain regions contributing to respiratory control. Prog Brain Res 107:145–156
23. Hoch CC, Reynolds CF, Nebes RD, Kupfer DJ, Berman SR, Campbell D (1989) Clinical significance of sleep-disordered breathing in Alzheimer's disease. Preliminary data. J Am Geriatr Soc 37:138–144
24. Huang XF, Paxinos G (1995) Human intermediate reticular zone: A cyto- and chemoarchitectonic study. J Comp Neurol 360:571–588
25. Hunter S (1985) The rostral mesencephalon in Parkinson's disease and Alzheimer's disease. Acta Neuropathol 68:53–58
26. Hyman BT (1997) The neuropathological diagnosis of Alzheimer's disease: clinical-pathological studies. Neurobiol Aging 18:27–32
27. Insausti R, Amaral DG, Cowan WM (1987) The entorhinal cortex of the monkey. III. Subcortical afferents. J Comp Neurol 264:396–408
28. Iqbal K, Braak H, Braak E, Grundke-Iqbal I (1993) Silver labeling of Alzheimer neurofibrillary changes and brain β-amyloid. J Histotechnol 16:335–342
29. Ishii T (1966) Distribution of Alzheimer's neurofibrillary changes in the brain stem and hypothalamus of senile dementia. Acta Neuropathol (Berl) 6:181–187
30. Kosik KS, Greenberg SM (1994) Tau protein and Alzheimer disease. In: Terry RD, Katzman R, Bick KL (eds) Alzheimer disease. Raven Press, New York, pp 335–344
31. Kremer B, Swaab D, Bots G, Fisser B, Ravid R, Roos, R (1991) The hypothalamic lateral tuberal nucleus in Alzheimer's disease. Ann Neurol 29:279–284
32. Landin K, Blennow K, Wallin A, Gottfries CG (1993) Low blood pressure and blood glucose levels in Alzheimer's disease. Evidence for a hypometabolic disorder. J Intern Med 233: 357–363
33. Martin GF, Holstege G, Mehler WR (1990) Reticular formation of the pons and medulla. In: Paxinos G (ed) The human central nervous system. Academic Press, San Diego, pp 203–220
34. Mercken M, Vandermeeren M, Lübke U, Six J, Boons J, Van de Voorde A, Martin JJ, Gheuens J (1992) Monoclonal antibodies with selective specifity for Alzheimer tau are directed against phosphatase-sensitive epitopes. Acta Neuropathol 84:265–272
35. Nieuwenhuys R (1996) The greater limbic system, the emotional motor system and the brain. Prog Brain Res 107:551–580
36. Ohm TG, Braak H (1988) The pigmented subpeduncular nucleus: a neuromelanin-containing nucleus in the human pontine tegmentum. Acta Neuropathol 77:26–32
37. Ohm TG, Müller H, Braak H, Bohl J (1995) Close-meshed prevalence rates of different stages as a tool to uncover the rate of Alzheimer's disease related neurofibrillary changes. Neuroscience 64:209–217
38. Olszewski J, Baxter D (1982) Cytoarchitecture of the human brain stem, 2nd edn. Karger, Basel
39. Parvizi J, Vanhoesen GW, Damasio A (1998) Severe pathological changes of parabrachial nucleus in Alzheimer's disease. Neuroreport 9:4151–4154
40. Paxinos G, Törk I, Halliday G, Mehler WR (1990) Human homologs to brainstem nuclei identified in other animals as revealed by acetylcholinesterase activity. In: Paxinos G (ed) The human central nervous system. Academic Press, San Diego, pp 149–202
41. Pearson RCA, Esiri MM, Hiorns RW, Wilcock GK, Powell TPS (1985) Anatomical correlates of the distribution of the pathological changes in the neocortex in Alzheimer disease. Proc Natl Acad Sci USA 82:4531–4534
42. Price JL (1998) Diagnostic criteria for Alzheimer's disease. Neurobiol Aging 18:67–70

43. Price DL, Thinakaran G, Borchelt DR, Martin LJ, Crain BJ, Sisodia SS, Troncoso JC (1998) Neuropathology of Alzheimer's disease and animal models. In:Markesbery WR (ed) Neuropathology of dementing disorders. Arnold, London, pp 121–141
44. Rebeck GW, Hyman BT (1993) Neuroanatomical connections and specific regional vulnerability in Alzheimer's disease. Neurobiol Aging 14:45–47
45. Rüb U, Braak H, Braak E, Schultz C, Sassin I, Ghebremedhin E, Thal D (1998) Development and distribution pattern of neurofibrillary changes in the raphe system and adjacent nuclei in Alzheimer's disease. Clin Neuropathol 17:250
46. Russchen FT, Amaral DG, Price JL (1985) The afferent connections of the substantia innominata in the monkey, macaca fascicularis. J Comp Neurol 242:1–27
47. Saper CB, German DC (1987) Hypothalamic pathology in Alzheimer's disease. Neurosci Lett 74:364–370
48. Saper CB, Wainer BH, German DC (1987) Axonal and transneuronal transport in the transmission of neurological disease: potential role in system degenerations, including Alzheimer's disease. Neuroscience 23:389–398
49. Sassin I, Schultz C, Thal DR, Rüb U, Arai K, Braak E, Braak H (2000) Evolution of Alzheimer's disease-related cytoskeletal changes in the basal nucleus of Meynert. Acta Neuropathol 100:259–269
50. Schofield P, Mayeux R (1998) Alzheimer's disease: clinical features, diagnosis and epidemiology. In: Markesbery WR (ed) Neuropathology of dementing disorders. Arnold, London, pp 89–105
51. Scinto LFM, Wu CK, Firla KM, Daffner KR, Saroff D, Geula C (1999) Focal pathology in the Edinger-Westphal nucleus explains pupillary hypersensitivity in Alzheimer's disease. Acta Neuropathol 97:557–564
52. Smithson KG, MacVicar BA, Hatton GI (1983) Polyethylene glycol embedding: a technique compatible with immunocytochemistry, enzyme histochemistry, histofluorescence and intracellular staining. J Neurosci Methods 7:27–41
53. Vitiello B, Veith RC, Molchan SE, Martinez RA, Lawlor BA. Radcliffe J, Hill JL, Sunderland T (1993) Autonomic dysfunction in patients with dementia of the Alzheimer type. Biol Psychiatry 34:428–433
54. Yamada M, Mehraein P (1977) Verteilungsmuster der senilen Veränderungen in den Hirnstammkernen. Folia Psychiat Neurol Jpn 31:219–224